Electronic Supplementary Material (ESI) for Inorganic Chemistry Frontiers.

Supporting Information (SI)

Design of Highly Stable Metal/ZSM-5 Catalyst for Shape-selective Alkylation of Toluene with Methanol to Para-xylene

He Han [a], Hong Yang [b],* Anfeng Zhang [a],* Limin Ren [c], Xiaowa Nie [a], Chaoqiu Chen[d], Min Liu [a], Chuan Shi [a], Chunshan Song [a, e], Xinwen Guo [a],*

[a]*State Key Laboratory of Fine Chemicals, Department of Catalytic Chemistry and Engineering, School of Chemical Engineering, Dalian University of Technology, Dalian, Liaoning Province,116024, P.R. China*
[b]*School of Engineering, The University of Western Australia, Perth, WA, 6009, Australia*
[c]*Zhang Dayu School of Chemistry, Dalian University of Technology, Dalian, Liaoning Province, 116024, P.R. China*
[d]*State Key Laboratory of Coal Conversion, Institute of Coal Chemistry, Chinese Academy of Sciences, Taiyuan, 030001, PR China*
[e]*Department of Chemistry, Faculty of Science, The Chinese University of Hong Kong, Shatin, NT, Hong Kong, 999077，P.R. China*

Corresponding Author

E-mail:

hong.yang@uwa.edu.au (H. Yang);

zhangaf@dlut.edu.cn (A. Zhang);

guoxw@dlut.edu.cn (X. Guo).

Table of content

SI-1 Summary of various zeolite catalysts for alkylation of toluene with methanol in literatures

SI-2 Crystal structure and textual properties of different catalysts

SI-3 Chemical properties of ZSM-5 catalysts without metals

SI-4 Loading of metal species over different M/MZ catalysts

SI-5 Reduction behavior of different MO_x loaded ZSM-5 catalysts

SI-6 States of metal species over M/MZ catalysts

SI-7 Catalytic performances and gas phase product distributions with time on stream over different catalysts

SI-8 Catalytic stability of M/MZ catalysts in (5%H_2 + 95%Ar) atmosphere

SI-9 Carbon mass balance over different catalysts

SI-10 Analysis of coke amounts

References

List of Figures and Tables

Table S1 Catalytic performance of zeolites with different topology structures for alkylation of toluene with methanol

Table S2 Catalytic performance of ZSM-5 zeolites with different modifications for alkylation of toluene with methanol (Results of our group)

Table S3 Catalytic performance of ZSM-5 zeolites with different modifications for alkylation of toluene with methanol (Results of other groups)

Table S4 Textural properties of HZ, MZ, and SiO_2@MZ catalysts determined by argon adsorption-desorption isotherms.

Table S5 Carbon mass balances of alkylation of toluene with methanol over different catalysts under H_2 atmosphere.

Figure S1. XRD patterns of the MO_x/ZSM-5 catalysts with different metal locations
Figure S2. Ar adsorption-desorption isotherms and pore size distribution curves of HZ, MZ, and SiO_2@MZ catalysts.
Figure S3. N_2 adsorption-desorption isotherms of the MO_x/ZSM-5 zeolite catalysts with different metal locations.
Figure S4. Chemical properties characterizations of HZ, MZ, and SiO_2@MZ catalysts.
Figure S5. H_2-TPR curves of different MO_x loaded ZSM-5 catalysts.
Figure S6. TEM images of Pt/MZ, Ni/MZ, and (Pt+Ni)/MZ catalysts.
Figure S7. HAADF-STEM images and EDS elemental mapping of Pt/MZ, Ni/MZ, and (Pt+Ni)/MZ catalysts.
Figure S8. Catalytic performance of HZ, MZ and SiO_2@MZ catalysts for alkylation of toluene with methanol in H_2 atmosphere.
Figure S9. Catalytic performance of M/MZ catalysts for alkylation of toluene with methanol in H_2 atmosphere.
Figure S10. Catalytic performance of M/SiO_2@MZ catalysts for alkylation of toluene with methanol in H_2 atmosphere.
Figure S11. Catalytic performance of SPM@(M/HZ) catalysts for alkylation of toluene with methanol in H_2 atmosphere.
Figure S12. Catalytic performance of SiO_2@(M/MZ) catalysts for alkylation of toluene with methanol in H_2 atmosphere.
Figure S13. Catalytic performance of M/MZ catalysts for alkylation of toluene with methanol in (5% H_2 + 95% Ar) atmosphere.
Figure S14. TG curves of different spent M/ZSM-5 catalysts after alkylation of toluene with methanol in the H_2 atmosphere.

SI-1 Summary of various zeolite catalysts for alkylation of toluene with methanol in literatures

Table S1-1 Catalytic performance of zeolites with different topology structures for alkylation of toluene with methanol

Zeolites	Topology	Ring size (T-atoms)	Maximum pore sizes for diffusion (Å)	Maximum pore sizes can be included (Å)	Modification	Reaction condition	Conversion of toluene (%)	Selectivity of *para*-xylene (%)	Selectivity of xylene (%)	Reference
SAPO-5	AFI	12,6,4	7.42	8.3	Unmodified	400℃; atmospheric pressure; F/W = 0.24 mol.g^{-1}.h^{-1}; n(T)/n(M) =2	16.0	25.0	-	1
β	BEA	12,6,5,4	5.95	6.68	Unmodified	300℃; atmospheric pressure; WHSV = 1038 h^{-1}; n(T)/n(M) =4	6.7	29.4	78.5	2
NU-87	NES	10,6,5,4	5.07	7.04	Unmodified	300℃; atmospheric pressure; WHSV = 576 h^{-1}; n(T)/n(M) =4	2.7	26.1	77.4	2
SSZ-33	CON	12,10,6,5,4	5.6	7.45	Unmodified	300℃; atmospheric pressure; WHSV = 372 h^{-1}; n(T)/n(M) =4	6.7	30.9	77.6	2
ZSM-5	MFI	10,6,5,4	4.7	6.36	Unmodified	300℃; atmospheric pressure; WHSV = 72 h^{-1}; n(T)/n(M) =4	3.1	59.3	93.6	2
Y	FAU	12 ,6,4	7.35	11.24	$NH4^+$-ion exchange	225℃; atmospheric pressure; F/W = 0.008 mol.g^{-1}.h^{-1}; n(T)/n(M) = 2;	> 28.9	51.0	-	3,4
Y					Ce-ion exchange		37.5	48.5	-	3,4
Mordenite	MOR	12,8,5,4	6.45	6.7	Unmodified	400℃; atmospheric pressure; Catalyst/feed = 5; n(T)/n(M) = 1;	49.6	24.2	27.6	5
ZSM-5							29.0	29.3	20.3	5
SSZ-33							42.0	24.4	18.3	5
TNU-9	TUN	10,8,6,5,4	5.39	8.46			43.3	25.0	24.1	5
ZSM-12	MTW	12,6,5,4	5.68	6.08	Unmodified	300℃; atmospheric pressure; LHSV = 2.5 h^{-1}; n(T)/n(M) = 0.5;	61.7	50.9	17.9	6
ZSM-12 /ZSM-5						300℃; atmospheric pressure; LHSV = 2.5 h^{-1}; n(T)/n(M) = 0.5;	44.0	89.3	83.5	6
SAPO-11	AEL	10,6,4	4.63	5.64	Unmodified	400℃; atmospheric pressure; WHSV = 3 h^{-1}; n(T)/n(M) = 2;	19.1	58.1	84.3	7

Table S1-2 Catalytic performance of zeolites with different topology structures for alkylation of toluene with methanol

Zeolites	Topology	Ring size (T-atoms)	Maximum pore sizes for diffusion (Å)	Maximum pore sizes can be included (Å)	Modification	Reaction condition	Conversion of toluene (%)	Selectivity of *para*-xylene (%)	Selectivity of xylene (%)	Reference
SAPO-31	ATO	12,6,4	5.49	5.74	Unmodified	400°C; atmospheric pressure; WHSV = 3 h^{-1}; n(T)/n(M) = 2;	32.1	37.3	69.5	7
SAPO-41	AFO	10,6,4	5.07	5.43		400°C; atmospheric pressure; WHSV = 4.5 h^{-1}; n(T)/n(M) = 2;	57.6	37.9	51.4	
MCM-22	MWW	10,6,5,4	4.92	9.69	Unmodified	250°C; atmospheric pressure; F/W = 0.48 mol.g^{-1}.h^{-1}; n(T)/n(M) = 1;	4.4	39.9	89.6	8
ITQ-2	MWW	10,6,5,4	4.92	9.69		250°C; atmospheric pressure; F/W = 0.44 mol.g^{-1}.h^{-1}; n(T)/n(M) = 1;	2.3	23.6	73.3	
MCM-22					Poisoned with collidine	250°C; atmospheric pressure; F/W = 0.47 mol.g^{-1}.h^{-1}; n(T)/n(M) = 1;	3.8	74.1	92.1	
ITQ-2						250°C; atmospheric pressure; F/W = 0.23 mol.g^{-1}.h^{-1}; n(T)/n(M) = 1;	0.6	80.0	100	
Mordenite					Unmodified	420°C; atmospheric pressure; WHSV = 2 h^{-1}; n(T)/n(M) = 2;	50.1	25.0	21.2	9,10
SAPO-11							31.2	25.0	83.4	
ZSM-5							43.9	25.0	50.2	
MCM-22							41.5	25.0	76.4	
ZSM-5					La-impregnation		20.0	91.0	50.2	
MCM-22							23.2	55.0	88.5	

Table S2 Catalytic performance of ZSM-5 zeolites with different modifications for alkylation of toluene with methanol (Results of our group)

Zeolites	Modification	Reaction condition	Conversion of toluene (%)	Selectivity of *para*-xylene (%)	Selectivity of xylene (%)	TOS (h)	Reference
Nano ZSM-5_2010 (Si/Al = 13, ~100 nm)	5 wt% P_2O_5+3 wt% MgO+ 6 wt% SiO_2+0.5 wt% Pt	T = 460℃; atmospheric pressure; WHSV = 2 h^{-1}; n(T)/n(M) = 2 $n(H_2)/n(H_2O)/n(T+M)$ = 8/8/1	23.0	98.0	>90	>500	[11]
Nano ZSM-5_2011 (Si/Al = 13, ~100 nm)	3 wt% SiO_2+5wt% P_2O_5+ 3 wt% MgO+3 wt% SiO_2+ 0.3 wt% Pt	T = 460℃; atmospheric pressure; WHSV = 2 h^{-1}; n(T)/n(M) = 2 $n(H_2)/n(H_2O)/n(T+M)$ = 8/8/1	23.0	98.0	>90	>500	[12]
Nano ZSM-5_2014 (Si/Al = 13, ~100 nm)	6 wt% SiO_2+5wt% P_2O_5+ 3 wt% MgO	T = 460℃; atmospheric pressure; WHSV = 2 h^{-1}; n(T)/n(M) = 8 $n(N_2)/n(H_2O)/n(T+M)$ = 8/8/1	11.0	98.0	>90	>1000	[13]
Nano ZSM-5_2017 (Si/Al = 13, ~100 nm)	6 wt% SiO_2+5wt% P_2O_5+ 3 wt% MgO+1 wt% SiO_2+ 0.15 wt% Pt	T = 460℃; pH_2 = 0.2 MPa; WHSV = 2.5 h^{-1}; n(T)/n(M) = 4 $n(H_2)/n(H_2O)/n(T+M)$ = 2/2/1	13.0	94.0	>90	>25	[14]
Hierarchical ZSM-5_2022 (Si/Al = 58, ~1000 nm)	Unmodified (HZ)	T = 460℃; pH_2 = 0.2 MPa; WHSV = 6 h^{-1}; n(T)/n(M) = 2 $n(H_2)/n(H_2O)/n(T+M)$ = 2/2/1	25.3	55.5	85.9	>60	This study
	6 wt% SiO_2+5wt% P_2O_5+ 3 wt% MgO (MZ)		20.4	94.9	90.2	<30	
	MZ+ 0.15 wt% Pt		18.9	94.7	96.7	>48	
	MZ+ 5 wt% Ni		19.5	95.7	92.9	>48	
	MZ+ (0.15 wt% Pt + 5 wt% Ni)		15.5	96.9	94.6	>58	
	MZ+ 0.15 wt% Pt	T = 460℃; $p(H_2+Ar)$= 0.2 MPa; WHSV = 6 h^{-1}; n(T)/n(M) = 2 $n(H_2+Ar)/n(H_2O)/n(T+M)$ = 2/2/1 H_2 concentration: 5%	22.2	93.2	90.9	<24	
	MZ+ 5 wt% Ni		15.3	94.3	91.3	<22	
	MZ+ (0.15 wt% Pt + 5 wt% Ni)		16.0	93.2	87.2	>100	

Table S3 Catalytic performance of ZSM-5 zeolites with different modifications for alkylation of toluene with methanol (Results of other groups)

Zeolites	Modification	Reaction condition	Conversion of toluene (%)	Selectivity of *para*-xylene (%)	Selectivity of xylene (%)	TOS (h)	Reference
Micro ZSM-5_2019 (Si/Al = 148, ~5 μm)	Unmodified Twin_HZSM-5	T = 470℃; atmospheric pressure; WHSV = 7.9 h^{-1}; n(T)/n(M) = 6 $n(H_2)/n(H_2O)/n$(T+M) = 7.1/5.3/1	10.2	99.0	-	220	[15]
Micro ZSM-5_2006 (Si/Al = 70, ~10 μm)	HZSM-5	T = 400℃; atmospheric pressure; WHSV = 0.3 h^{-1}; n(T)/n(M) = 1 n(gas)/$n(H_2O)$/n(T+M) not mentioned	53.7	50.1	88.8	1	[16]
	Silicalite/H-ZSM-5		49.9	99.9	92.4		
Micro ZSM-5_2006 (Si/Al = 108, ~3 μm)	HZSM-5	T = 400℃; atmospheric pressure; WHSV = 1 h^{-1}; n(T)/n(M) = 1 n(gas)/$n(H_2O)$/n(T+M) not mentioned	42.7	63.1	91.1	1	[17]
	Silicalite/H-ZSM-5		37.2	98.9	95.2		
ZSM-5_2007 (Si/Al = 40)	HZSM-5	T = 440℃; atmospheric pressure; WHSV = 2.5 h^{-1}; n(T)/n(M) = 8 $n(H_2)/n(H_2O)/n$(T+M) = 2/1/1	6.4	23.3	-	-	[18]
	10% B/ZSM-5		5.5	99.9			
	3% B/ZSM-5		5.0	99.9		66	
	10% Mg/ZSM-5		6.5	92.7		-	
ZSM-5_2005 (Si/Al = 40)	10% Mg/ZSM-5	T = 440℃; atmospheric pressure; WHSV = 11.6 h^{-1}; n(T)/n(M) = 8 $n(H_2)/n(H_2O)/n$(T+M) = 6/1/1	10~12	99.9	-	-	[19]
ZSM-5_2014 (Si/Al = 75)	HZSM-5	T = 420℃; atmospheric pressure; WHSV = 2 h^{-1}; n(T)/n(M) = 2 $n(H_2O)$/ n(T+M) = 2/3	37.5	24.0	51.2	0.2	[20]
	Si/PLaHZSM-5		24.2	97.6	84.6	0.2	
			15.0	97.0	84.6	120	
ZSM-5_2013 (Si/Al = 25, ~1 μm)	3% P-13% SiO_2-1% Ni-S-HZSM-5	T = 460℃; atmospheric pressure; WHSV = 2 h^{-1}; n(T)/n(M) = 2 H_2 atmosphere	31.0	91.0	-	5	[21]
ZSM-5_2019 (Si/Al = 25, ~1 μm)	C-ZSM-5	T = 420℃; 0.3 MPa; WHSV = 4 h^{-1}; n(T)/n(M) = 6 $n(H_2)/n(H_2O)/n$(T+M) = 10/10/1	12.4	23.8	-	-	[22]
	2Si-C-ZSM-5		12.3	27.2			
	4Si-C-ZSM-5		8.2	96.8			

SI-2 Crystal structure and textual properties of metal-loaded MZ catalysts

SI-2.1 Crystal structure

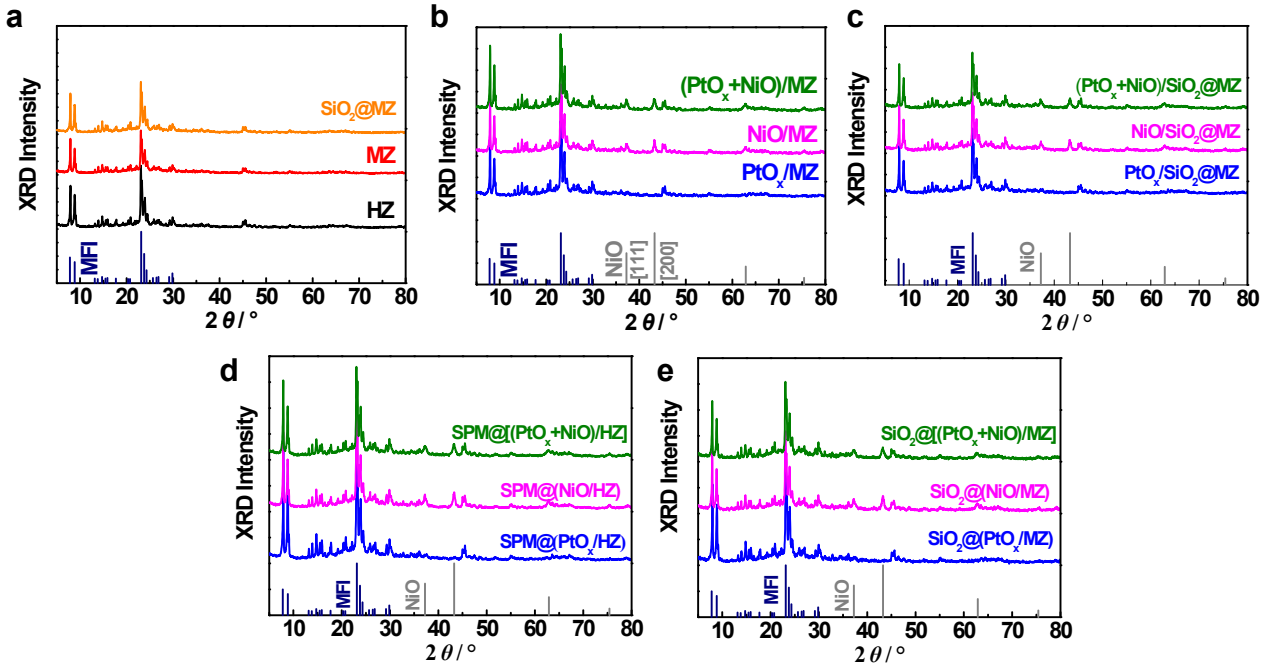

Figure S1. XRD patterns of the MO_x/ZSM-5 catalysts with different metal locations, a) HZ, MZ, and SiO_2@MZ, b) M/MZ, c) M/SiO_2@MZ, d) SPM@(M/HZ), and e) SiO_2@(M/MZ).

SI-2.2 Textural properties

Ar adsorption-desorption isotherms are used to analyze the micro- and meso- porosity of the HZ, MZ, and SiO_2@MZ catalysts. The measured isotherms and the textural properties extracted from the isotherms are provided in Figure S2 and Table S4. As reported previously[23], HZ, MZ, and SiO_2@MZ exhibit similar type IV argon adsorption-desorption isotherms (Figure S2a). As seen in Figure S2b, SiO_2 deposition results in negligible changes to argon adsorbed volume at p/p_0 = 0.01 indicating the microporosity of SiO_2@MZ and MZ are almost similar. In addition, Figure S2c shows the micropore size distribution curves indicating that zeolite samples exhibit a strong peak centered at ~ 0.5 nm which is consistent with the maximum diameter (0.47 nm) for molecule diffusion in MFI zeolites (Data from the website of International Zeolite Association). Figure S2d indicates that zeolite catalysts also possess certain amount of mesopores (around 5~20 nm).

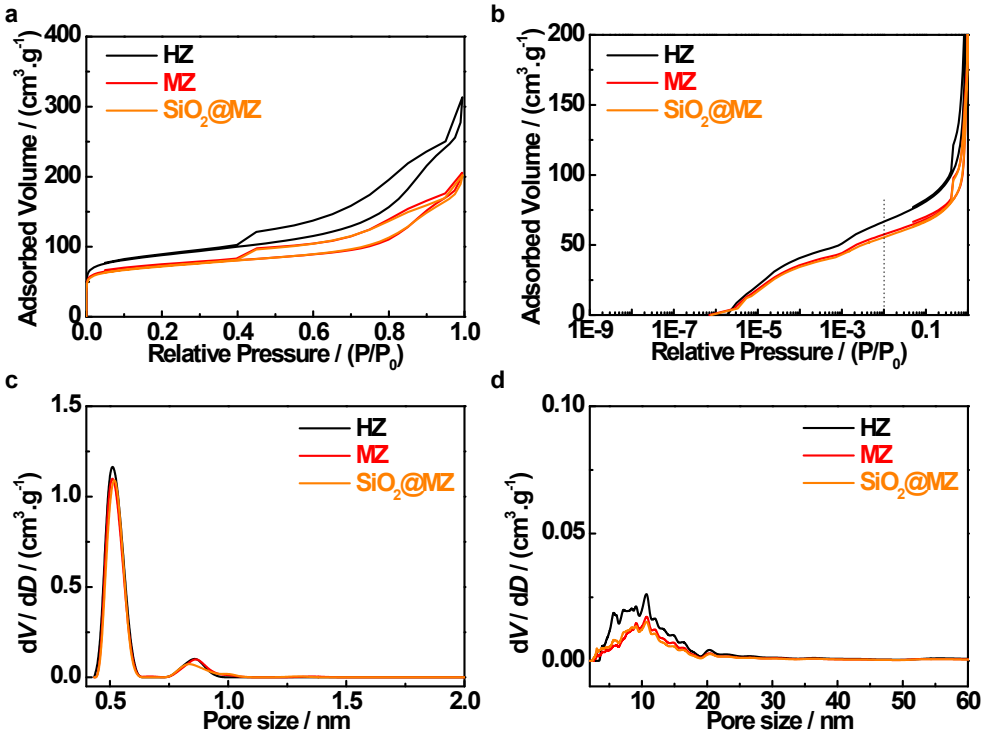

Figure S2. Ar adsorption-desorption isotherms of HZ, MZ, and SiO_2@MZ catalysts in linear (a) and logarithmic scales (b) and corresponding micropore (c) and mesopore (d) size distributions curves of HZ, MZ, and SiO_2@MZ catalysts.

Table S4. Textural properties of HZ, MZ, and SiO_2@MZ catalysts determined by argon adsorption-desorption isotherms.

Catalysts	S_{BET}	S_{micro}	S_{meso}	V_{total}	V_{micro}	V_{meso}
	($m^2.g^{-1}$)			($cm^3.g^{-1}$)		
HZ[a]	323	183	139	0.37	0.08	0.30
MZ[a]	240	178	62	0.22	0.07	0.15
SiO_2@MZ	233	165	67	0.21	0.06	0.15

[a] Results are cited from the literature.

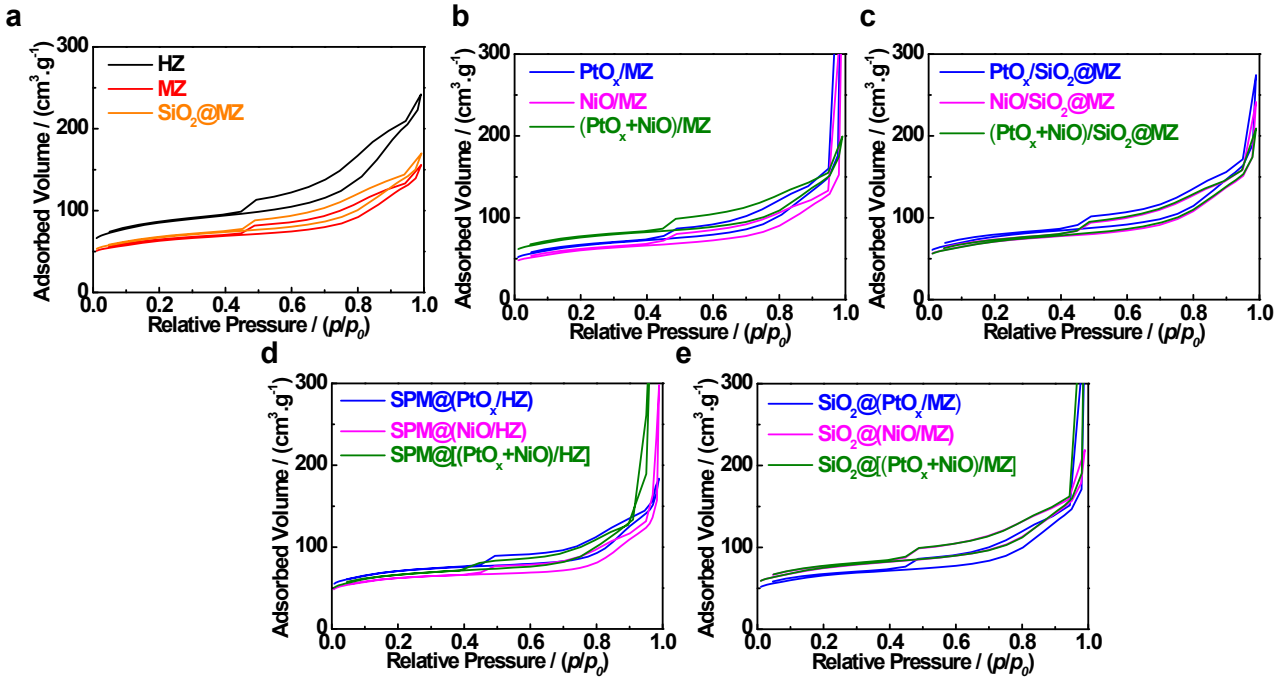

Figure S3. N_2 adsorption-desorption isotherms of the MO_x/ZSM-5 zeolite catalysts with different metal locations, a) HZ, MZ, and SiO_2@MZ, b) M/MZ, c) M/SiO_2@MZ, d) SPM@(M/HZ), and e) SiO_2@(M/MZ).

SI-3 Chemical properties of ZSM-5 zeolites without metals

Figure S4d shows that the Al_{2p} signals decreased continuously by SPM surface modification and SiO_2 coating. This result supports that 1 wt% SiO_2 coating passivates the external aluminum sites.

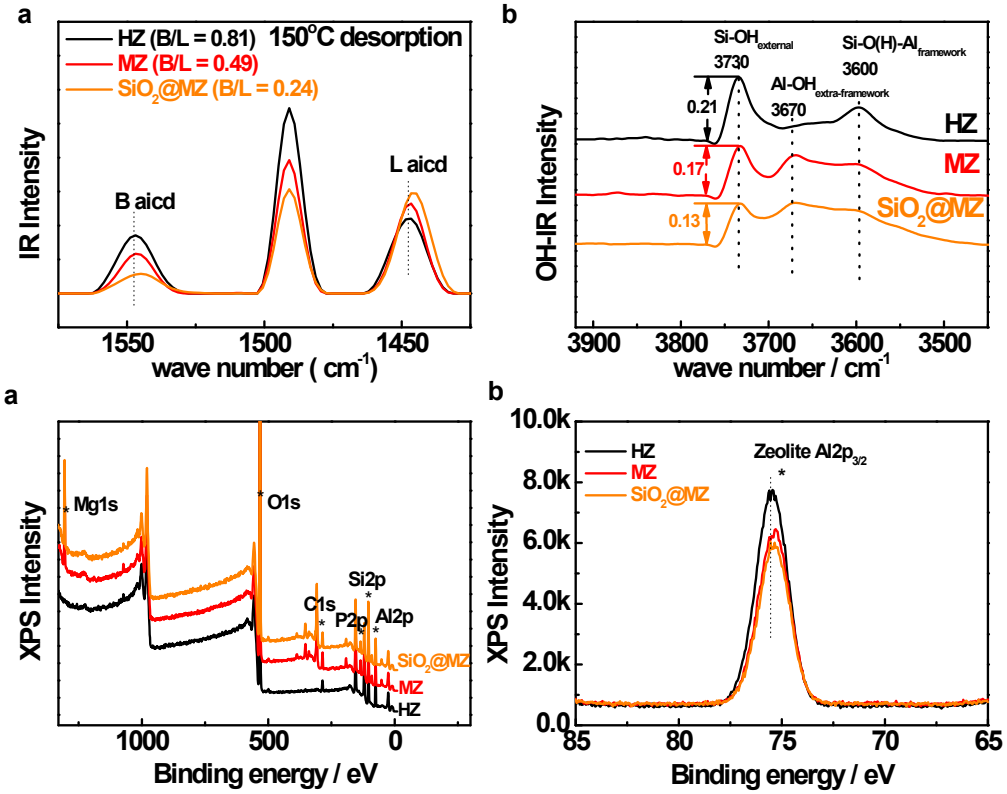

Figure S4. Chemical properties characterizations of HZ, MZ, and SiO_2@MZ catalysts: a) FT-IR spectra of pyridine adsorption at 150 °C, b) FT-IR spectra in the O—H stretching region, c) XPS survey spectra, and d) Al_{2p} XPS spectra.

SI-4 Loading of metal species over different M/MZ catalysts

The loading of Ni for Ni/MZ and (Pt+Ni)/MZ are determined by XRF in our previous work which are 5.0 wt% and 4.9%, respectively[23]. The loading of Pt for Pt/MZ and (Pt+Ni)/MZ are also determined by ICP in our previous work which are 0.07 wt% and 0.12%, respectively[23].

SI-5 Reduction behavior of different MO_x loaded ZSM-5 catalysts

Temperature programmed reduction (TPR) of H_2 is performed on a CHEMBET 3000 chemical adsorber (Quantachrome, USA) to analyze the natures of metal species. In a typical H_2-TPR measurement, about 0.1 g of the sample is degassed in helium at 500 ^oC for 1 h, cooled to 25 ^oC and then exposed to a hydrogen-argon mixture (5% H_2 + 95% Ar) for 30 min. The TPR curves are obtained at a heating rate of 10 ^oC min^{-1} from 25 ^oC to 900 ^oC. The adsorbed hydrogen is detected by gas chromatography equipped with a thermal conductivity detector.

Figure S5 presents the H_2-TPR curves of the as-prepared MO_x loaded catalysts. This testing is done to reveal the reduction behavior of MO_x, including the peak position (corresponding to the H_2 consumption temperature) and the peak area (corresponding to the H_2 consumption amount).

Note that no H_2 consumption peak is observed for any sole PtO_x loaded catalysts, likely due to very low Pt loading with some PtO_x already in reduced (i.e., Pt) form[23].

Figure S5a presents the H_2-TPR curves for MO_x/MZ as reported in our published work[23], it is included here to assist the explanation of results for other catalysts. As seen in Figures S5a-b, MZ and SiO_2@MZ do not show any H_2 consumption peak. The reduction of NiO over NiO/MZ occurs in two stages. The first stage ranges from 400 to 700 ^oC while the second stage extends to over 880 ^oC. These two stages may be attributed to the reduction of large NiO crystals and those small NiO clusters have strong interaction with the supports. Compared with NiO/MZ, there are two strong NiO reduction peaks for NiO/SiO_2@MZ at 618 ^oC and 680 ^oC, respectively. In addition, there is a weak NiO reduction peak over 800 ^oC. This indicates a significant narrowing of reduction temperature range. This seems to suggest that the overall reduction of NiO on SiO_2 surface becomes easier than on MZ. Furthermore, just as in the case on MZ, the reduction of mixed (PtO_x+NiO) oxide occurs at the relatively lower temperatures than sole NiO/SiO_2@MZ. In addition, the total H_2 consumption amounts of the two catalysts are similar.

When MO_x is covered by either SPM or SiO_2, the H_2 consumption amount decreases noticeably as seen in Figure S5c-d, while the peak temperatures seem to remain similar to their relevant counterparts. This reduction of H_2 consumption amount is particularly significant for the SPM covered samples. This indicates that the SPM coating hinders the effective access of H_2 to MO_x species.

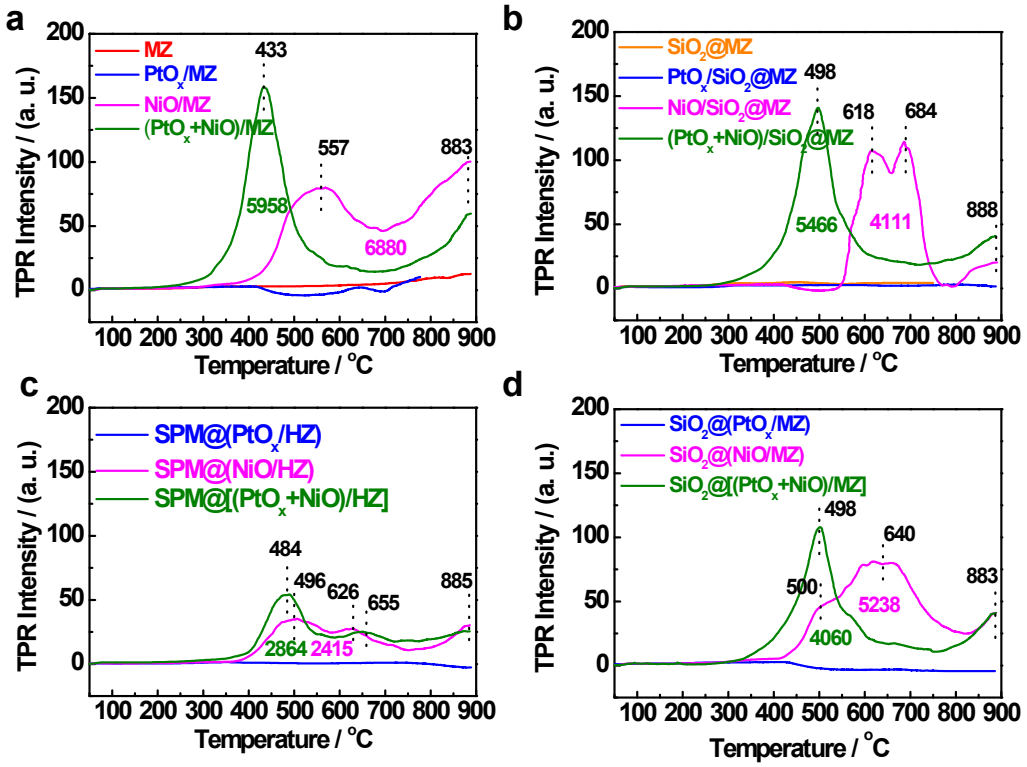

Figure S5. H_2-TPR curves of different MO_x loaded ZSM-5 catalysts: a) MZ and MO_x/MZ, b) SiO_2@MZ and MO_x/SiO_2@MZ, c) SPM@(MO_x/HZ), and d) SiO_2@(MO_x/MZ). The number under each curve represents the total hydrogen consumption amount with the unit of $mmol.g^{-1}$. The dashed vertical lines mark the hydrogen consumption peak temperatures.

SI-6 States of metal species over M/MZ catalysts

Transmission electron microscopy (TEM) images are taken on a Field Emission Transmission Electron Microscope JEM-F200 instrument (JEOL Company) at an acceleration voltage of 200 kV. The samples for TEM analysis are prepared by dipping the carbon-coated copper grids into an ethanol solution of the sample and allowed to dry under ambient conditions.

Figure S6 presents the TEM images of the Pt/MZ, Ni/MZ and (Pt+Ni)/MZ catalysts which are *in-situ* reduced by H_2 at 500 ^oC. As seen in Figure S6a, a metal nanoparticle with the size of ca 100×60 nm is located on the rim of zeolite particle. High resolution TEM images in Figure S6b indicates that this metal nanoparticle should be Al_2Pt since the lattice fringes of $Al_2Pt(111)$ (d = 0.350 nm) and $Al_2Pt(220)$ (d = 0.206 nm) are observed. We infer that Al_2Pt is formed due to the interaction between PtO_x and Al_2O_3 with the treatment of H_2 reduction. Note that Al_2O_3 is introduced as the binder for zeolites. Figure S6c shows that an individual Ni nanoparticle with the size of ca 30×25 nm. The lattice fringes of Ni(111) (d = 0.208 nm) is shown in Figure S6d. According to (Pt+Ni)/MZ, Figure S6e and f show a NiPt nanoparticle with the size of ca 40×35 nm. The lattice fringe of NiPt (200) (d = 0.193 nm) is shown in Figure S6f. We find that there are some interlaced lattice fringes in this nanoparticle which may attributed to NiPt alloy. But we also find that part of the metal nanoparticles over (Pt+Ni)/MZ should be attributed to pure Ni.

The distributions of Pt or/and Ni metals over zeolites could be further confirmed by the dark field TEM images and EDS elemental mapping which are shown in Figure S7. The images of Figure S7e and f indicate that Pt and Ni sites over (Pt+Ni)/MZ catalysts are intimately mixed.

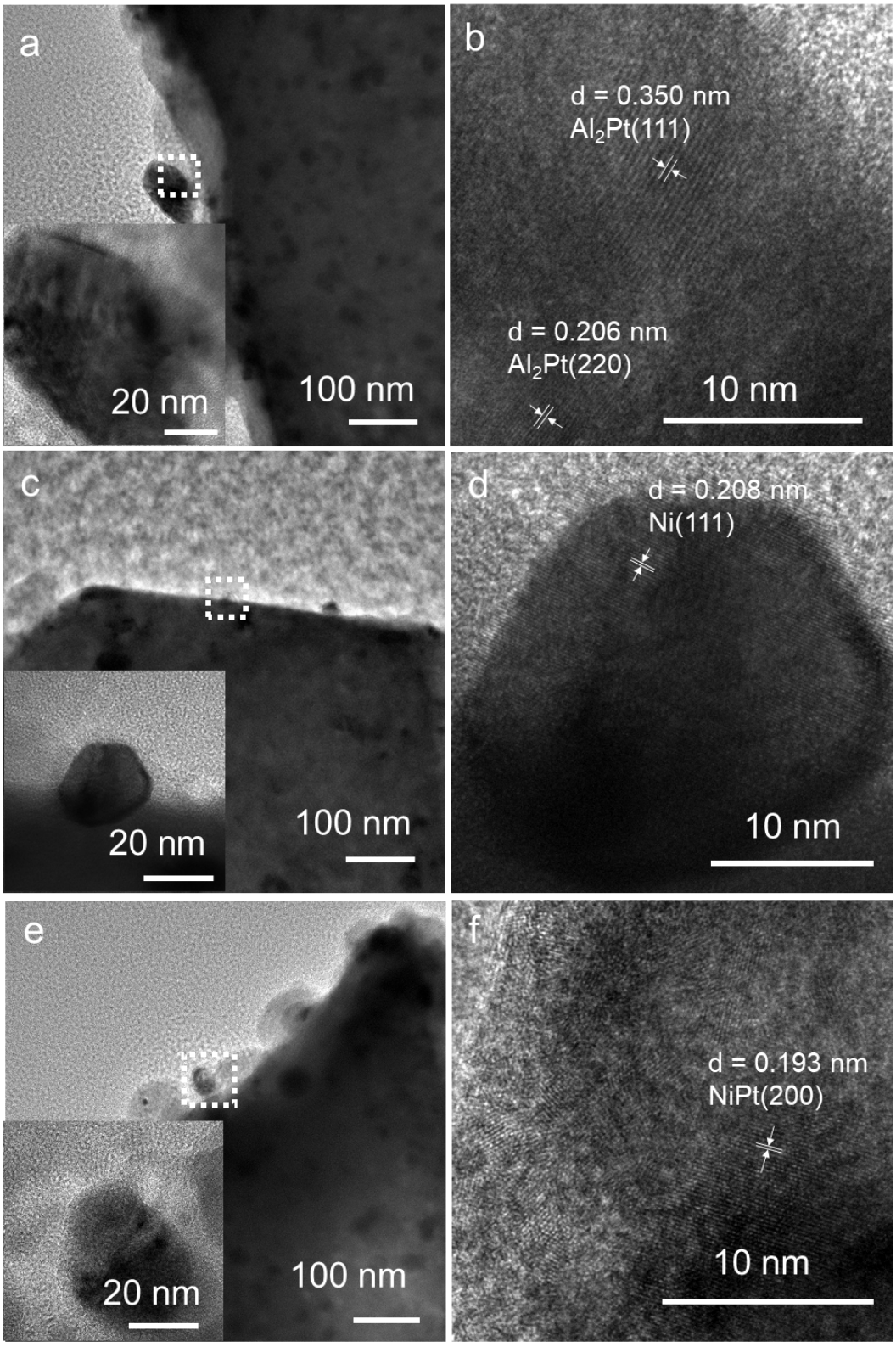

Figure S6. TEM images of Pt/MZ(a and b), Ni/MZ(c and d) and (Pt+Ni)/MZ(e and f) catalysts which are reduced by H_2. The insert images in Figure a), c), and e) show the entire metal nanoparticles. The dashed-squares in Figure a), c), and e) highlight the metal nanoparticles, as confirmed by HRTEM images provided in Figure b), d) and f).

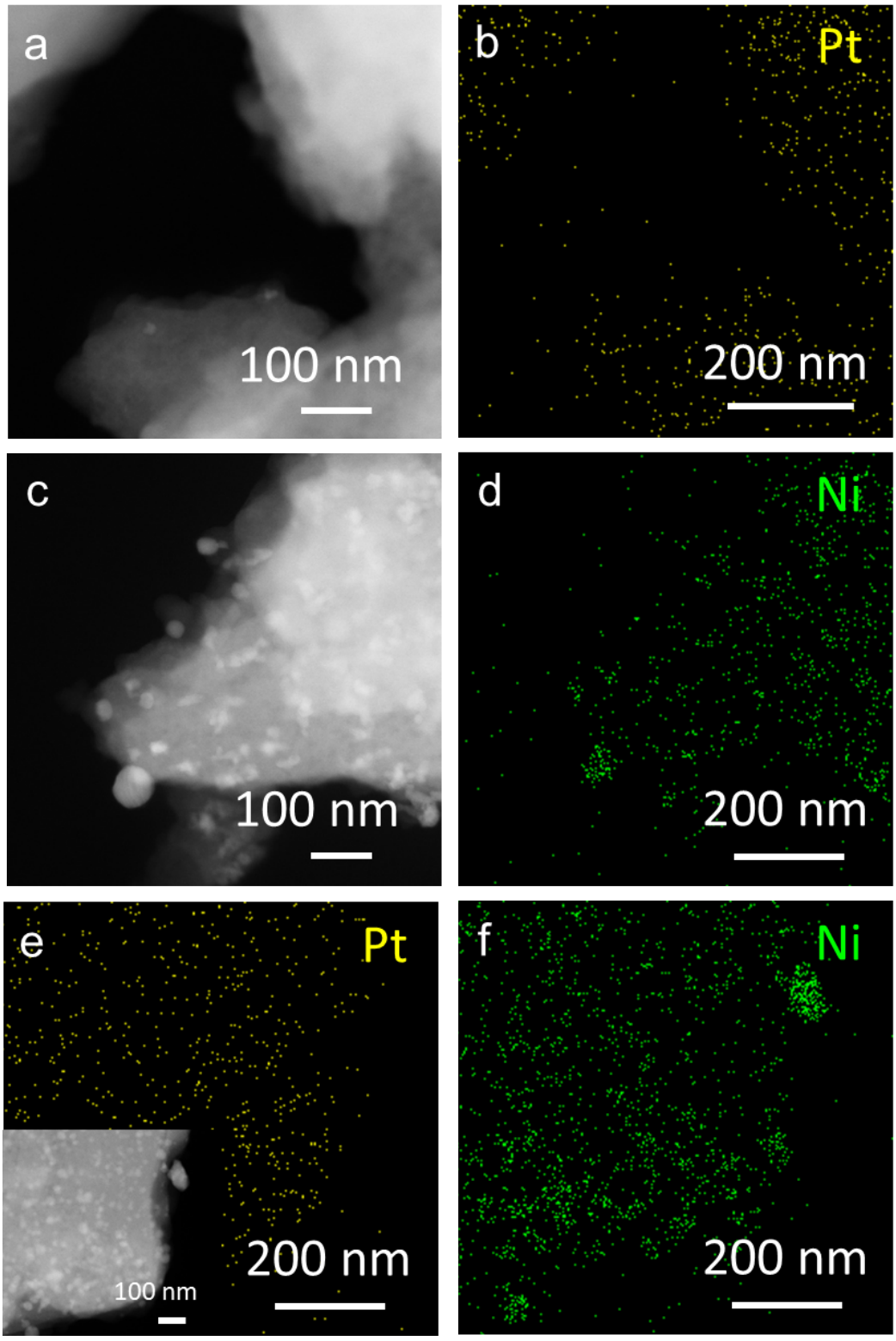

Figure S7. HAADF-STEM images and EDS elemental mapping of Pt/MZ (a, b), Ni/MZ (c, d), and (Pt+Ni)/MZ (e, f). The insert image in figure 'e' is the HAADF-STEM image of (Pt+Ni)/MZ.

SI-7 Catalytic performances and gas phase product distributions with time on stream over different catalysts

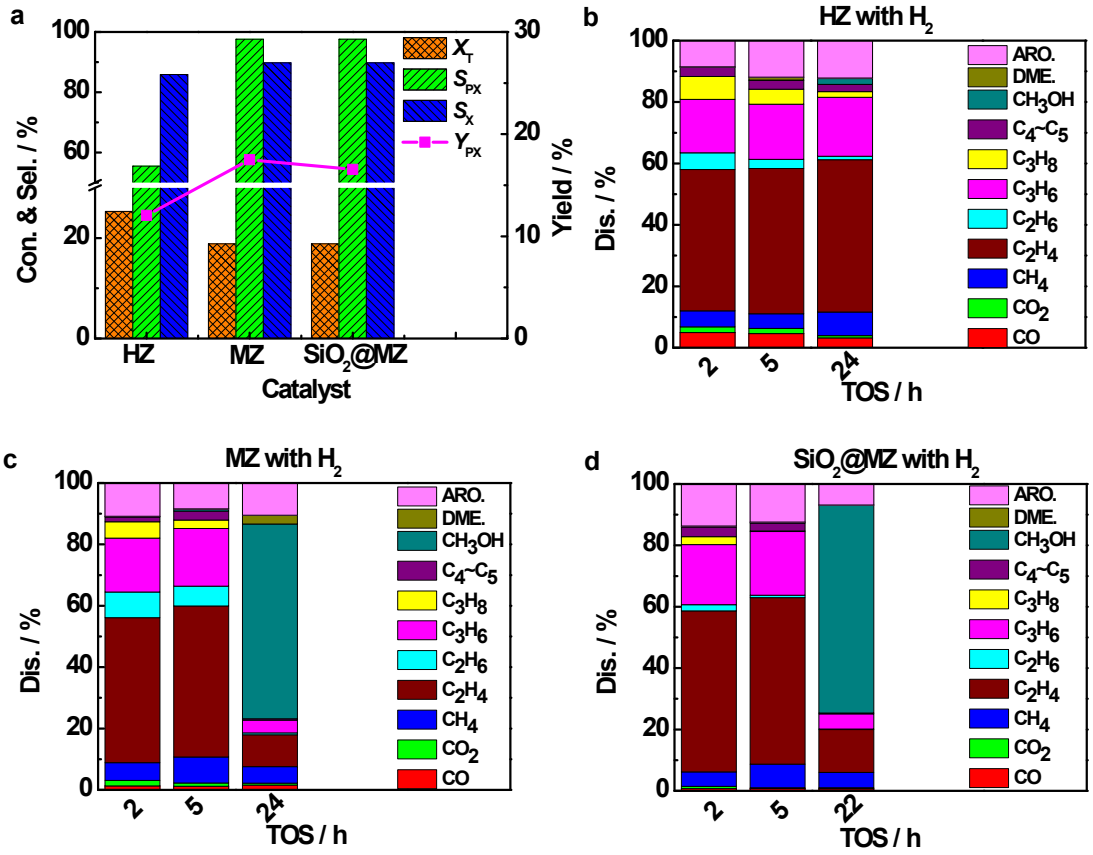

Figure S8. Catalytic performance of HZ, MZ and SiO_2@MZ catalysts for alkylation of toluene with methanol in H_2 atmosphere (Note that HZ and MZ is reported in our previous work[23].). a) the catalytic activity and selectivity obtained from the highest X_T, c-d) gas phase product distributions with time on stream (Reaction conditions: T = 460 °C, p = 0.2 MPa, $WHSV$ = 6 h^{-1}, n_T/n_M = 2/1, $n_{H2}/n_{H2O}/n_{(T+M)}$ = 2/2/1).

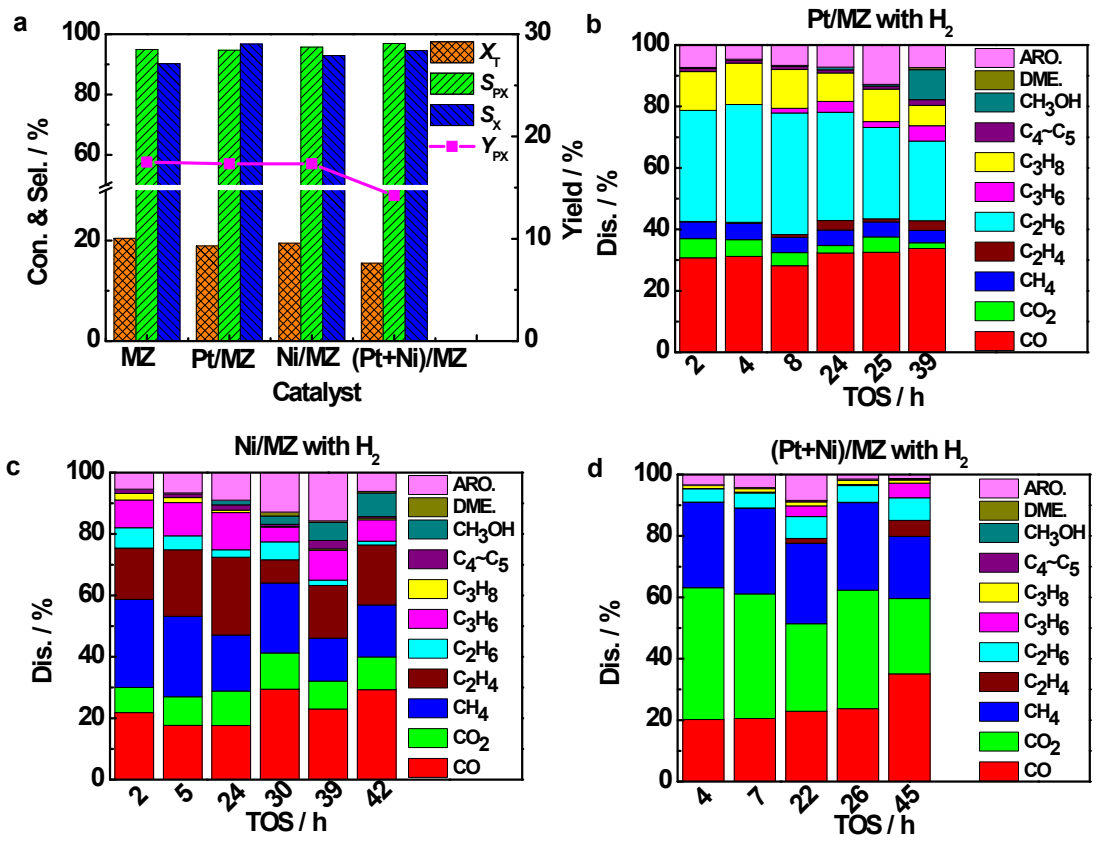

Figure S9. Catalytic performance of M/MZ catalysts for alkylation of toluene with methanol in H_2 atmosphere (Note that M/MZ are reported in our previous work[23].), a) the catalytic activity and selectivity obtained from the highest X_T, c-d) gas phase product distributions with time on stream (Reaction conditions: T = 460 °C, p = 0.2 MPa, $WHSV$ = 6 h^{-1}, n_T/n_M = 2/1, $n_{H2}/n_{H2O}/n_{(T+M)}$ = 2/2/1).

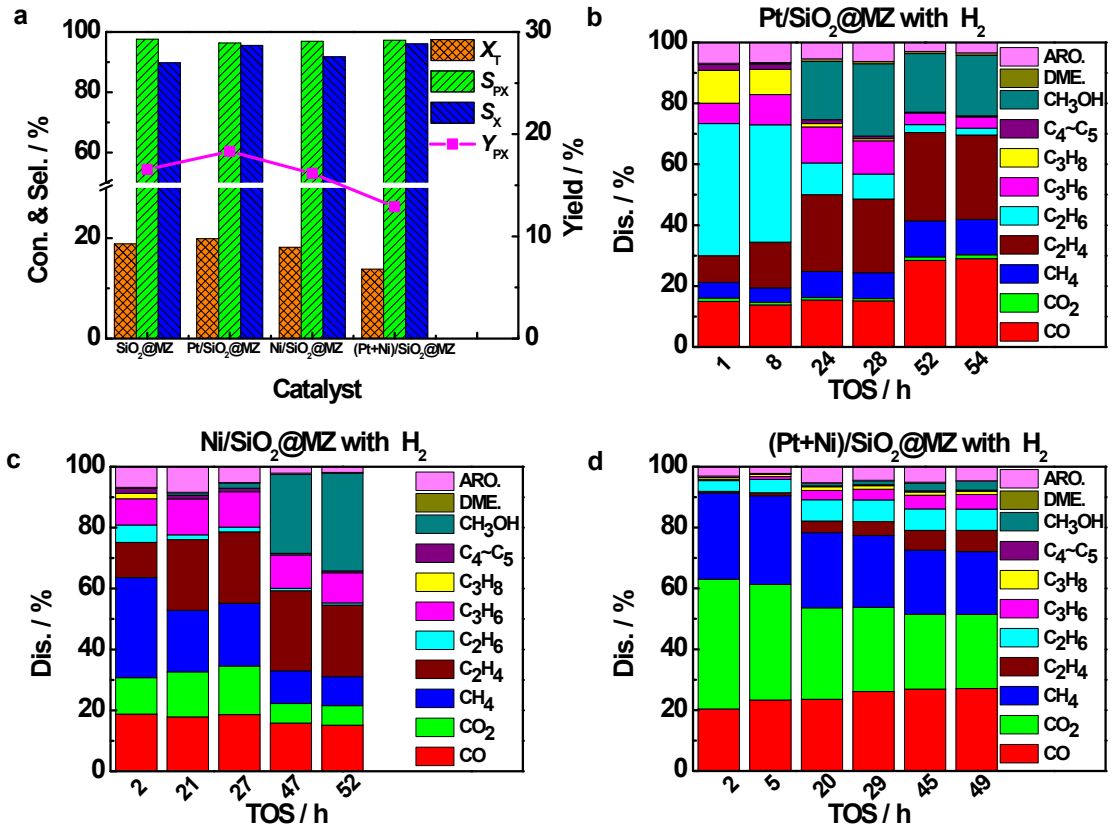

Figure S10. Catalytic performance of M/SiO_2@MZ catalysts for alkylation of toluene with methanol in H_2 atmosphere. a) the catalytic activity and selectivity obtained from the highest X_T, c-d) gas phase product distributions with time on stream (Reaction conditions: T = 460 °C, p = 0.2 MPa, $WHSV$ = 6 h^{-1}, n_T/n_M = 2/1, $n_{H2}/n_{H2O}/n_{(T+M)}$ = 2/2/1).

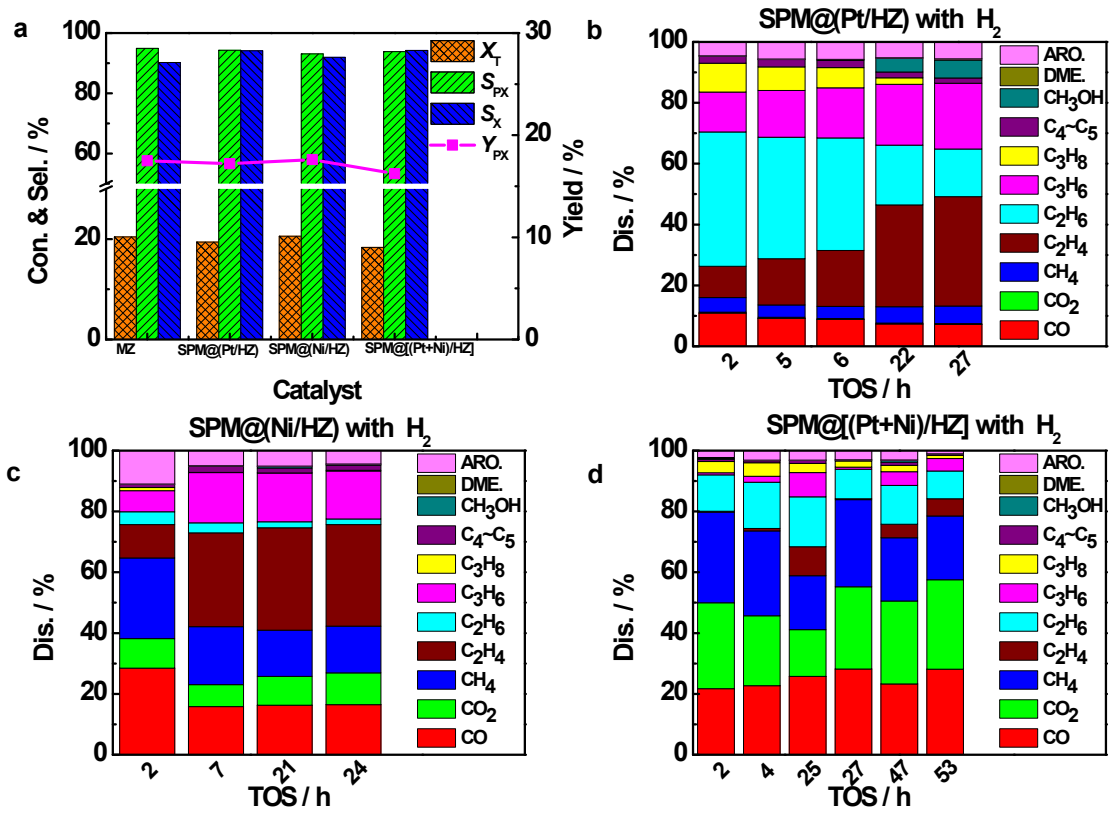

Figure S11. Catalytic performance of SPM@(M/HZ) catalysts for alkylation of toluene with methanol in H_2 atmosphere. a) the catalytic activity and selectivity obtained from the highest X_T, c-d) gas phase product distributions with time on stream (Reaction conditions: T = 460 °C, p = 0.2 MPa, $WHSV$ = 6 h^{-1}, n_T/n_M = 2/1, $n_{H2}/n_{H2O}/n_{(T+M)}$ = 2/2/1).

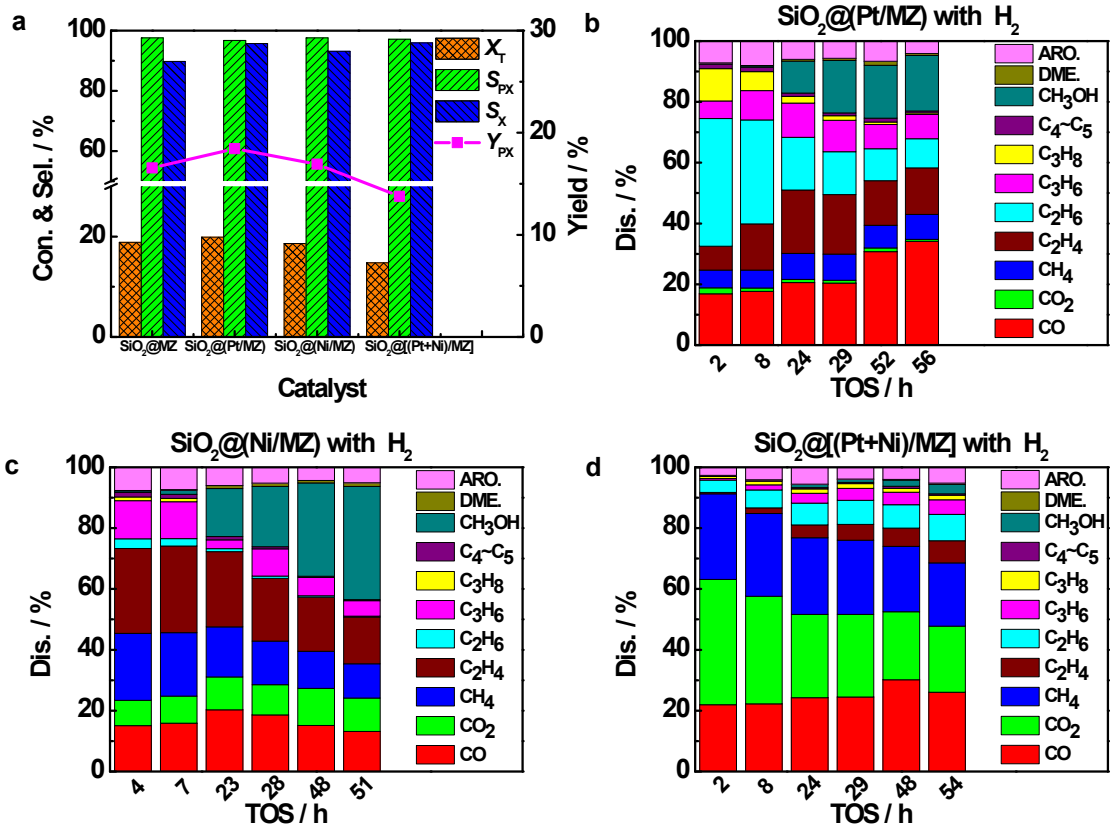

Figure S12. Catalytic performance of SiO_2@(M/MZ) catalysts for alkylation of toluene with methanol in H_2 atmosphere. a) the catalytic activity and selectivity obtained from the highest X_T, c-d) gas phase product distributions with time on stream (Reaction conditions: T = 460 °C, p = 0.2 MPa, $WHSV$ = 6 h^{-1}, n_T/n_M = 2/1, $n_{H2}/n_{H2O}/n_{(T+M)}$ = 2/2/1).

SI-8 Catalytic stability of M/MZ catalysts in (5%H_2 + 95%Ar) atmosphere

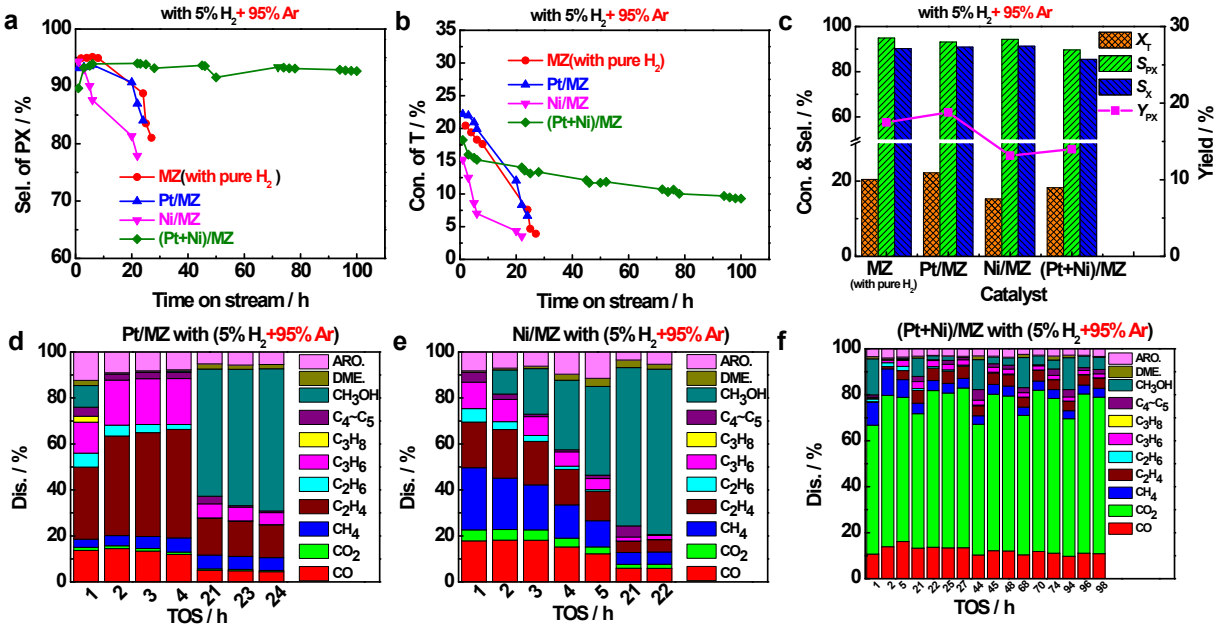

Figure S13. Catalytic performance of M/MZ catalysts for alkylation of toluene with methanol in (5% H_2 + 95% Ar) atmosphere. a) conversion of toluene (X_T) with time on stream, b) selectivity of *para*-xylene (S_{PX}) with time on stream, c) the catalytic activity and selectivity obtained from the highest X_T, d-f) gas phase product distributions with time on stream (Reaction conditions: T = 460 °C, p = 0.2 MPa, $WHSV$ = 6 h^{-1}, n_T/n_M = 2/1, $n_{(5\%H2+95\%Ar)}/n_{H2O}/n_{(T+M)}$ = 2/2/1).

SI-9 Carbon mass balance over different catalysts

The carbon mass balances of alkylation of toluene with methanol over different catalysts in H_2 atmosphere are calculated and provided in Table S5. Note that the carbon mass balance is calculated based on following assumptions

(i) All aromatic products are generated from toluene;
(ii) All carbon oxides, paraffins and olefins are generated from methanol;
(iii) The amounts of methanol and toluene converted to coke are negligible.

Thus, the gaseous and liquid product distributions can now be calculated from equation S1 as following:

$$\frac{[aromatic\ in\ gas\ product] + [aromatic\ in\ liquid\ product]}{\begin{matrix}[unreacted\ methanol\ in\ gas\ \ product] + [unreacted\ methanol\ in\ liquid\ \ product] + \\ [\ methanol\ converted\ to\ gas\ byproduct] + [methanol\ reacted\ with\ toluene]\end{matrix}} = \frac{[toluene\ in\ feed]}{[methnoal\ in\ feed]} \quad (S1)$$

Table S5-1 Carbon mass balances of alkylation of toluene with methanol over different catalysts under H_2 atmosphere.

Gaseous product	Liquid product	Feed	Carbon mass balances over different catalysts (mol%)		
			HZ	MZ	SiO_2@MZ
CO	-	0	0.4	0.1	0.1
CO_2	-	0	0.2	0.2	0.1
CH_4	-	0	0.5	0.7	0.6
C_2H_2	-	0	4.1	5.4	6.8
C_2H_6		0	0.5	1.0	0.3
C_3H_6		0	1.6	2.0	2.5
C_3H_8		0	0.7	0.6	0.3
C_4-C_5		0	0.3	0.2	0.4
CH_3OH	-	0	0	0	0
DME	-	0	0	0	0
Aromatic	-	0	0.8	1.2	1.8
-	$C6^-$	0	1.3	2.1	1.1
	CH_3OH	33.3	0	0.2	0.2
-	Benzene	0	0.1	0.1	0.1
-	Toluene	66.7	67.0	68.7	70.0
-	Ethylbenzene	0	0	0.1	0.1
-	*p*-Xylene	0	10.8	15.1	13.9
	m-Xylene	0	6.2	0.6	0.2
	o-Xylene	0	2.5	0.2	0.1
-	Ethyltoluene	0	1.0	1.2	1.2
-	Trimethylbenzene	0	1.5	0.1	0.1
-	$C9^+$	0	0.6	0.2	0.2
Total		100	100	100	100
$U_{\text{m-aromatics}}$ (%)		-	58.5	45.8	40.2
$U_{\text{m-olefins}}$ (%)		-	29.6	40.9	50.2
$U_{\text{m-paraffins}}$ (%)		-	10.4	12.4	8.9
$U_{\text{m-COx}}$ (%)		-	1.4	0.9	0.5
$U_{\text{m-aromatics + olefins + paraffins + COx}}$ (%)		-	100	99.9	99.9

Table S5-2 Carbon mass balances of alkylation of toluene with methanol over different catalysts under H_2 atmosphere.

Gaseous product	Liquid product	Carbon mass balances over different catalysts (mol%)					
		Pt/MZ	Ni/MZ	(Pt+Ni)/MZ	Pt/SiO_2@MZ	Ni/SiO_2@MZ	(Pt+Ni)/SiO_2@MZ
CO	-	4.8	3.5	4.9	1.9	3.4	5.2
CO_2	-	1.0	1.3	10.3	0.1	2.2	10.9
CH_4	-	0.8	4.6	6.7	0.7	5.9	7.2
C_2H_2	-	0	2.7	0	1.1	2.1	0.1
C_2H_6		5.6	1.1	1.0	5.6	1.0	0.9
C_3H_6		0	1.4	0	0.9	1.6	0.1
C_3H_8		2.0	0.3	0.2	1.4	0.3	0.2
C_4-C_5		0.2	0.2	0	0.3	0.3	0
CH_3OH	-	0	0	0	0	0	0
DME	-	0	0	0	0	0	0
Aromatic	-	1.1	0.9	0.8	0.9	1.2	0.8
-	$C6^-$	1.3	1.4	0.6	1.3	1.0	0.4
	CH_3OH	0.2	0.2	0.2	0.2	0.2	0.2
-	Benzene	0.1	0.1	0.1	0.1	0.2	0.1
-	Toluene	67.2	66.3	63.5	68.4	66.1	63.8
-	Ethylbenzene	0	0	0	0	0	0
-	*p*-Xylene	14.4	14.3	10.7	15.6	13.1	9.5
	m-Xylene	0.6	0.5	0.2	0.5	0.3	0.2
	o-Xylene	0.2	0.2	0.1	0.1	0.1	0.1
-	Ethyltoluene	0.2	0.7	0.4	0.5	0.8	0.2
-	Trimethylbenzene	0.2	0.1	0.1	0.1	0.1	0.1
-	$C9^+$	0	0.1	0	0	0	0.0
Total		100	100	100	100	100	100
$U_{\text{m-aromatics}}$ (%)		39.4	42.1	32.3	41.9	38.1	27.9
$U_{\text{m-olefins}}$ (%)		0.1	24.3	0.3	11.8	22.2	1.7
$U_{\text{m-paraffins}}$ (%)		46.1	21.5	26.1	41.2	25.5	26.4
$U_{\text{m-COx}}$ (%)		14.2	12.1	41.2	5.0	13.9	44.0
$U_{\text{m-aromatics + olefins + paraffins + COx}}$ (%)		99.8	100.0	99.9	99.9	99.8	99.9

Table S5-3 Carbon mass balances of alkylation of toluene with methanol over different catalysts under H_2 atmosphere.

Gaseous product	Liquid product	Carbon mass balances over different catalysts (mol%)					
		SPM@(Pt/HZ)	SPM@(Ni/HZ)	SPM@[(Pt+Ni)/HZ]	SiO_2@(Pt/MZ)	SiO_2@(Ni/MZ)	SiO_2@[(Pt+Ni)/MZ]
CO	-	1.3	5.3	4.5	2.3	2.3	5.5
CO_2	-	0	1.8	5.9	0.3	1.3	10.3
CH_4	-	0.6	4.9	6.2	0.8	3.4	7.0
C_2H_2	-	1.2	2.0	0.1	1.1	4.4	0.1
C_2H_6		5.3	0.8	2.5	5.7	0.5	1.0
C_3H_6		1.6	1.3	0.1	0.8	2.0	0.1
C_3H_8		1.1	0.2	0.8	1.4	0.2	0.2
C_4-C_5		0.3	0.2	0.2	0.2	0.2	0
CH_3OH	-	0	0	0	0	0.1	0
DME	-	0	0	0.1	0	0	0
Aromatic	-	0.5	2.0	0.5	1.0	1.2	0.7
-	$C6^-$	1.4	0.9	0.5	1.3	1.3	0.4
	CH_3OH	0.2	0.1	0.2	0.2	0.2	0.2
-	Benzene	0.1	0.1	0.3	0.1	0.1	0.1
-	Toluene	69.7	63.9	64.7	68.3	67.5	63.6
-	Ethylbenzene	0	0	0	0	0	0
-	*p*-Xylene	14.8	14.2	12.1	15.4	14.0	10.0
	m-Xylene	0.7	0.8	0.7	0.4	0.3	0.2
	o-Xylene	0.2	0.3	0.2	0.1	0.1	0.1
-	Ethyltoluene	0.5	0.8	0.2	0.5	0.7	0.2
-	Trimethylbenzene	0.2	0.3	0.1	0.1	0.1	0.1
-	$C9^+$	0.2	0.1	0	0	0.1	0
Total		100	100	100	100	100	100
$U_{\text{m-aromatics}}$ (%)		41.9	43.4	34.6	41.4	40.0	29.2
$U_{\text{m-olefins}}$ (%)		17.2	19.6	1.4	10.8	36.2	1.7
$U_{\text{m-paraffins}}$ (%)		37.6	19.4	36.7	41.7	14.6	26.3
$U_{\text{m-COx}}$ (%)		3.2	17.5	26.9	6.1	9.1	42.7
$U_{\text{m-aromatics + olefins + paraffins + COx}}$ (%)		100.0	99.9	99.6	100.0	99.9	99.9

SI-10 Analysis of coke amount

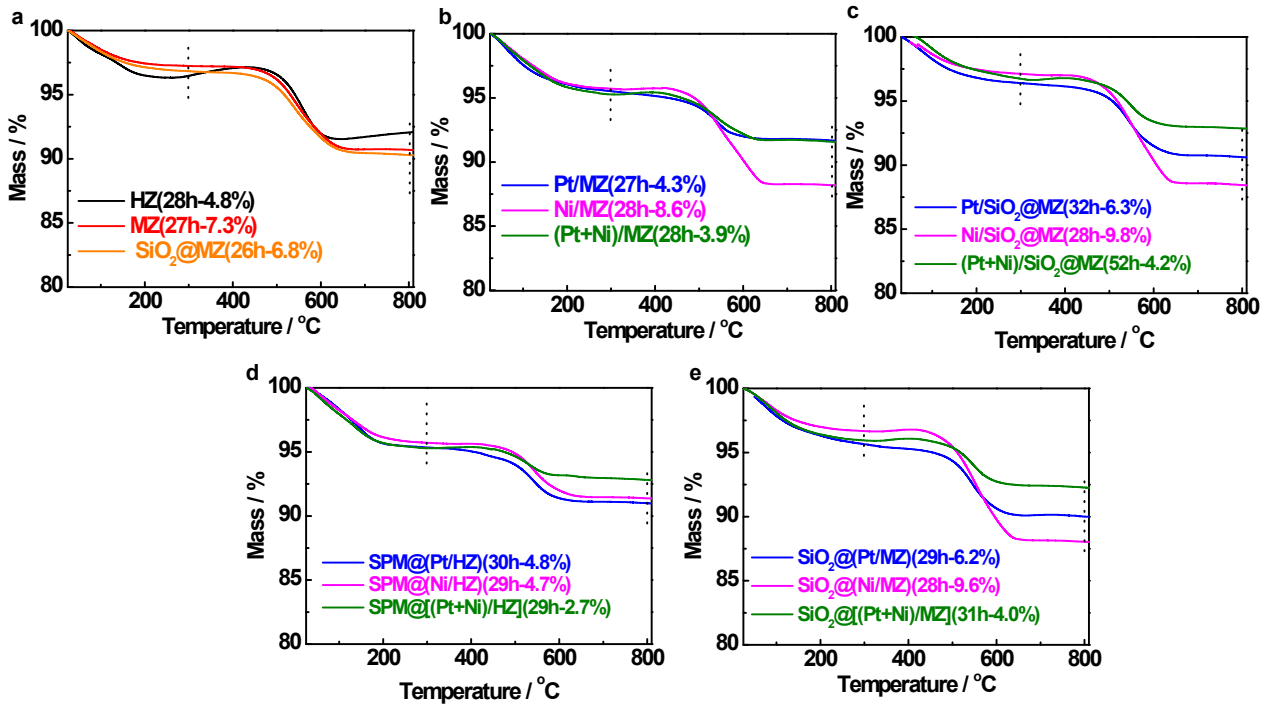

Figure S14. TG curves of different spent M/ZSM-5 catalysts after alkylation of toluene with methanol in the H_2 atmosphere, a) HZ, MZ, and SiO_2@MZ, b) M/MZ, c) M/SiO_2@MZ, d) SPM@(M/HZ), and e) SiO_2@(M/MZ) (The reaction periods endured by the spent catalysts and their coke amount are indicated in their brackets).

References

1 T. Masukawa, T. Komatsu and T. Yashima, Alkylation of toluene on HSAPO-5 with various Si concentrations, *Zeolites*, 1997, **19**, 429-433.

2 F. J. Llopis, G. Sastre and A. Corma, Xylene isomerization and aromatic alkylation in zeolites NU-87, SSZ-33, β, and ZSM-5: molecular dynamics and catalytic studies, *J. Catal.*, 2004, **227**, 227-241.

3 T. Yashima, H. Ahmad, K. Yamazaki, M. Katsuta and N. Hara, Alkylation on synthetic zeolites: I. Alkylation of toluene with methanol, *J. Catal.*, 1970, **16**, 273-280.

4 T. Yashima, K. Yamazaki, H. Ahmad, M. Katsuta and N. Hara, Alkylation on synthetic zeolites: II. Selectivity of p-xylene formation, *J. Catal.*, 1970, **17**, 151-156.

5 A. Baduraig, T. Odedairo and S. Al-Khattaf, Disproportionation and Methylation of Toluene with Methanol Over Zeolite Catalysts, *Top. Catal.*, 2010, **53**, 1446-1456.

6 P. N. Joshi, P. S. Niphadkar, P. A. Desai, R. Patil and V. V. Bokade, Toluene Alkylation to Selective Formation of p-Xylene over Co-Crystalline ZSM-12/ZSM-5 Catalyst, *J. Nat. Gas Chem.*, 2007, **16**, 37-41.

7 A. M. Prakash, S. V. V. Chilukuri, R. P. Bagwe, S. Ashtekar and D. K. Chakrabarty, Silicoaluminophosphate molecular sieves SAPO-11, SAPO-31 and SAPO-41: synthesis, characterization and alkylation of toluene with methanol, *Microporous Mater.*, 1996, **6**, 89-97.

8 S. Inagaki, K. Kamino, E. Kikuchi and M. Matsukata, Shape selectivity of MWW-type aluminosilicate zeolites in the alkylation of toluene with methanol, *Appl. Catal. A-Gen.*, 2007, **318**, 22-27.

9 Z. Zhu, Q. Chen, Z. Xie, W. Yang and C. Li, The roles of acidity and structure of zeolite for catalyzing toluene alkylation with methanol to xylene, *Microporous Mesoporous Mater.*, 2006, **88**, 16-21.

10 Z. Zhu, Q. Chen, W. Zhu, D. Kong and C. Li, Catalytic performance of MCM-22 zeolite for alkylation of toluene with methanol, *Catal. Today*, 2004, **93-95**, 321-325.

11 Y. Zhao, H. Wu, W. Tan, M. Zhang, M. Liu, C. Song, X. Wang and X. Guo, Effect of metal modification of HZSM-5 on catalyst stability in the shape-selective methylation of toluene, *Catal. Today*, 2010, **156**, 69-73.

12 Y. Zhao, W. Tan, H. Wu, A. Zhang, M. Liu, G. Li, X. Wang, C. Song and X. Guo, Effect of Pt on stability of nano-scale ZSM-5 catalyst for toluene alkylation with methanol into p-xylene, *Catal. Today*, 2011, **160**, 179-183.

13 W. Tan, M. Liu, Y. Zhao, K. Hou, H. Wu, A. Zhang, H. Liu, Y. Wang, C. Song and X. Guo, Para-selective methylation of toluene with methanol over nano-sized ZSM-5 catalysts: Synergistic effects of surface modifications with SiO2, P2O5 and MgO, *Microporous Mesoporous Mater.*, 2014, **196**, 18-30.

14 Y. Wang, M. Liu, A. Zhang, Y. Zuo, F. Ding, Y. Chang, C. Song and X. Guo, Methanol Usage in Toluene Methylation over Pt Modified ZSM-5 Catalyst: Effects of Total Pressure and Carrier Gas, *Ind. Eng. Chem. Res.*, 2017, **56**, 4709-4717.

15 C. Wang, L. Zhang, X. Huang, Y. Zhu, G. K. Li, Q. Gu, J. Chen, L. Ma, X. Li, Q. He, J. Xu, Q. Sun, C. Song, M. Peng, J. Sun and D. Ma, Maximizing sinusoidal channels of HZSM-5 for high shape-selectivity to p-xylene, *Nat. Commun.*, 2019, **10**, 4348.

16 D. Van Vu, M. Miyamoto, N. Nishiyama, Y. Egashira and K. Ueyama, Selective formation of para-xylene over H-ZSM-5 coated with polycrystalline silicalite crystals, *J. Catal.*, 2006, **243**, 389-394.

17 M. Miyamoto, T. Kamei, N. Nishiyama, Y. Egashira and K. Ueyama, Single Crystals of ZSM-5/Silicalite Composites. Advanced Materials, *Adv. Mater.*, 2005, **17**, 1985-1988.

18 J. P. Breen, R. Burch, M. Kulkarni, D. Mclaughlin, P. J. Collier and S. E. Golunski, Improved selectivity in the toluene alkylation reaction through understanding and optimising the process variables, *Appl. Catal. A-Gen.*, 2007, **316**, 53-60.

19 J. Breen, R. Burch, M. Kulkarni, P. Collier and S. Golunski, Enhanced para-Xylene Selectivity in the Toluene Alkylation Reaction at Ultralow Contact Time, *J. Am. Chem. Soc.*, 2005, **127**, 5020-5021.

20 Y. Bi, Y. Wang, Y. Wei, Y. He, Z. Yu, Z. Liu and L. Xu, Improved Selectivity toward Light Olefins in the Reaction of Toluene with Methanol Over the Modified HZSM-5 Catalyst, *ChemCatChem*, 2014, **6**, 713-718.

21 P. Lu, Z. Fei, L. Li, X. Feng, W. Ji, W. Ding, Y. Chen, W. Yang and Z. Xie, Effects of controlled SiO2 deposition and phosphorus and nickel doping on surface acidity and diffusivity of medium and small sized HZSM-5 for para-selective alkylation of toluene by methanol, *Appl. Catal. A-Gen.*, 2013, **453**, 302-309.

22 J. Li, W. Ji, M. Liu, G. Zhao, W. Jia and Z. Zhu, New insight into the alkylation-efficiency of methanol with toluene over ZSM-5: Microporous diffusibility significantly affects reacting-pathways, *Microporous Mesoporous Mater.*, 2019, **282**, 252-259.

23 H. Han, A. Zhang, L. Ren, X. Nie, M. Liu, Y. Liu, C. Shi, H. Yang, C. Song and X. Guo, Coke-resistant (Pt + Ni)/ZSM-5 catalyst for shape-selective alkylation of toluene with methanol to para-xylene, *Chem. Eng. Sci.*, 2022, **252**, 117529.